© 2016. Published by The Company of Biologists Ltd | Journal of Cell Science (2016) 129, 1198-1209 doi:10.1242/jcs.182006

RESEARCH ARTICLE

Soluble LILRA3 promotes neurite outgrowth and synapses formation through a high-affinity interaction with Nogo 66

Hongyan An[1], Merryn Brettle[2], Terry Lee[1], Benjamin Heng[3], Chai K. Lim[3], Gilles J. Guillemin[3], Megan S. Lord[4], Enrico Klotzsch[5], Carolyn L. Geczy[1], Katherine Bryant[1], Thomas Fath[2,*] and Nicodemus Tedla[1,*,‡]

ABSTRACT

Inhibitory proteins, particularly Nogo 66, a highly conserved 66-amino-acid loop of Nogo A (an isoform of RTN4), play key roles in limiting the intrinsic capacity of the central nervous system (CNS) to regenerate after injury. Ligation of surface Nogo receptors (NgRs) and/or leukocyte immunoglobulin-like receptor B2 (LILRB2) and its mouse orthologue the paired immunoglobulin-like receptor B (PIRB) by Nogo 66 transduces inhibitory signals that potently inhibit neurite outgrowth. Here, we show that soluble leukocyte immunoglobulin-like receptor A3 (LILRA3) is a high-affinity receptor for Nogo 66, suggesting that LILRA3 might be a competitive antagonist to these cell surface inhibitory receptors. Consistent with this, LILRA3 significantly reversed Nogo-66-mediated inhibition of neurite outgrowth and promoted synapse formation in primary cortical neurons through regulation of the ERK/MEK pathway. LILRA3 represents a new antagonist to Nogo-66-mediated inhibition of neurite outgrowth in the CNS, a function distinct from its immune-regulatory role in leukocytes. This report is also the first to demonstrate that a member of LILR family normally not expressed in rodents exerts functions on mouse neurons through the highly homologous Nogo 66 ligand.

KEY WORDS: Leukocyte immunoglobulin-like receptor A3, Nogo 66, PIRB, Cortical neuron, Neurite outgrowth, Synapse

INTRODUCTION

Leukocyte immunoglobulin-like receptor A3 (LILRA3) is a soluble member of a family of activating and inhibitory immune-regulatory cell surface receptors primarily expressed on leukocytes and that is increasingly recognised as a key regulator of the threshold and amplitude of leukocyte activation (Borges and Cosman, 2000; Brown et al., 2004; An et al., 2010; Tedla et al., 2011). LILRA3 is unique in that it lacks transmembrane and cytoplasmic domains, thus is an exclusively secreted protein (Borges and Cosman, 2000). Although LILRA3 functions have not been fully elucidated, it shares high structural similarity to cell surface LILRs, including the inhibitory LILRB2 (Borges and Cosman, 2000; Brown et al., 2004), and hence might act as a soluble antagonist through shared ligands. However, natural ligands for LILRA3 have not been fully identified; a knowledge gap that has severely hindered understanding of its functions. LILRs are selectively conserved in humans and primates and are the most conserved among genes located within the leukocyte receptor complex on chromosome 19, implying important functions (Martin et al., 2002). There are no rodent homologues, although paired immunoglobulin-like receptor B (PIRB), considered the murine orthologue of human LILRB2, regulates leukocyte functions through similar signalling cascades (Martin et al., 2002).

Nogo 66 is a highly conserved 66-amino-acid surface membrane loop of the reticulon family of proteins that include Nogo A, Nogo B and Nogo C (isoforms of RTN4), and is crucial for several vital inhibitory roles of Nogo proteins (Chen et al., 2000; GrandPré et al., 2000; Prinjha et al., 2000; Fry et al., 2007; Rodriguez-Feo et al., 2007; David et al., 2008; Kritz et al., 2008; Schwab, 2010; Wright et al., 2010). In Nogo A, Nogo 66 is a potent inhibitor of axonal regeneration and neurite outgrowth after central nervous system (CNS) injury that acts through interaction with its traditional receptors (NgR1 and NgR2, also known as RTN4R and RTN4RL2, respectively) (Fournier et al., 2001; Schwab, 2010) and the newly discovered inhibitory immunoglobulin-like receptors, human LILRB2 and its murine orthologue PIRB (Atwal et al., 2008; Adelson et al., 2012). Although studies are limited, the more ubiquitously expressed Nogo B inhibits inflammation (Wright et al., 2010) and decreases vascular injury (Rodriguez-Feo et al., 2007; Kritz et al., 2008). Nogo C is expressed in the CNS and skeletal muscle, but functions are unknown (Schwab, 2010).

Limited studies show that LILRA3 interacts with some major histocompatibility complex (MHC) class I molecules, albeit with low-binding affinities (μM amounts), but there is a lack of functional data (Jones et al., 2011). These deficiencies might be due in part to the existence of an alternative high-affinity LILRA3 ligand(s) or due to the use of unsuitably glycosylated and/or truncated fusion LILRA3 proteins (Jones et al., 2011). Our aim was to identify cell surface proteins that interact with mammalian-produced, properly glycosylated, full-length recombinant LILRA3 (Lee et al., 2013) and define their functions. After initial screening of numerous primary cells and cell lines, we found human monocytes exhibited high-affinity binding to recombinant LILRA3 (Lee et al., 2013). Plasma membrane proteins from these cells were used in a new proteomic approach to identify two new [Nogo 66 and 67-kDa laminin receptor (also known as RPSA)] and one known MHC class I (HLA-B) molecules as candidate high-affinity LILRA3-binding proteins. Of particular interest was the interaction between Nogo 66 and LILRA3, as this was unexpected given that Nogo 66 is commonly associated with inhibition of neurite outgrowth in the CNS (GrandPré et al., 2000; Schwab, 2010). LILRA3 and Nogo 66 binding was therefore confirmed by

[1]Inflammation and Infection Research Centre, School of Medical Sciences, Department of Pathology, UNSW, Sydney, New South Wales 2052, Australia. [2]Neurodegeneration and Repair Unit, School of Medical Sciences, Department of Anatomy, UNSW, Sydney, New South Wales 2052, Australia. [3]Faculty of Medicine and Health Sciences, Department of Biomedical Sciences, Macquarie University, Sydney, 2109, Australia. [4]Graduate School of Biomedical Engineering, UNSW, Sydney, New South Wales 2052, Australia. [5]EMBL Australia Node in Single Molecule Science, School of Medical Sciences, ARC Centre of Excellence in Advanced Molecular Imaging, The University of New South Wales, Sydney, New South Wales 2052, Australia.
*These authors contributed equally to this work

‡Author for correspondence (n.tedla@unsw.edu.au)

Received 15 October 2015; Accepted 26 January 2016

Journal of Cell Science

Journal of Cell Science (2016) 129, 1198-1209 doi:10.1242/jcs.182006

several independent methods including surface plasmon resonance (SPR), co-immunoprecipitation studies and biochemical assays. We show that LILRA3 binding to Nogo 66 was high affinity, saturable and specific. Importantly, LILRA3 potently reversed Nogo-66-mediated inhibition of neurite outgrowth in human and mouse primary cortical neurons *in vitro* and increased numbers of synaptic contacts, likely through regulation of the ERK/MEK pathway. This tantalising discovery points to new LILRA3 functions in the CNS, distinct from its proposed regulatory role in leukocytes. We propose that soluble LILRA3 might function as an antagonist against the closely related cell surface inhibitory receptors LILRB2 and PIRB by competitively binding to a shared Nogo 66 ligand. Reversal of Nogo-mediated inhibition of neurite outgrowth by endogenous LILRA3 might have implications in CNS disease states where Nogo A is a major contributor to the inhibitory microenvironment leading to failed regeneration after neuro-axonal damage.

RESULTS

Identification of Nogo 66 as a new ligand for soluble LILRA3

Nano liquid chromatography tandem mass spectrometry (LC-MS/MS) of in-gel trypsin digested peptides from co-immunoprecipitation experiments using placental alkaline phosphatase (AP)-tagged recombinant LILRA3 as bait identified three LILRA3-binding proteins with high MASCOT scores in three independent experiments (Fig. S1). Two proteins, Nogo A (four to seven peptide matches; mascot score of 189–277) and the 67-kDa laminin receptor (two to five peptide matches; mascot score of 112–115) were identified as potential new binding partners, whereas HLA-B (two to five peptide matches; mascot score of 109–113) is known to bind LILRA3 (Jones et al., 2011). At least three of the four to seven peptide sequences identified as Nogo proteins were part of the highly conserved 66-amino-acid surface membrane loop of the reticulon family of proteins that include Nogo A, Nogo B and Nogo C (Fig. S1). These proteins were not present in control samples when alkaline phosphatase control protein was used as bait, indicating specificity.

Nogo 66 is a high-affinity ligand for soluble LILRA3

High-affinity binding of LILRA3 to Nogo 66 was confirmed using four independent approaches. First, SPR steady-state equilibrium analysis indicated that soluble LILRA3 maintained picomolar affinity binding (K_D=2.21±0.45×10^{-10} M, n=3) to chip-immobilised recombinant Nogo 66 (500–600 relative units) (Fig. 1A). Second, recombinant Nogo 66 specifically bound to concanavalin A (ConA)–Sepharose-immobilised untagged recombinant LILRA3 but not to control Sepharose

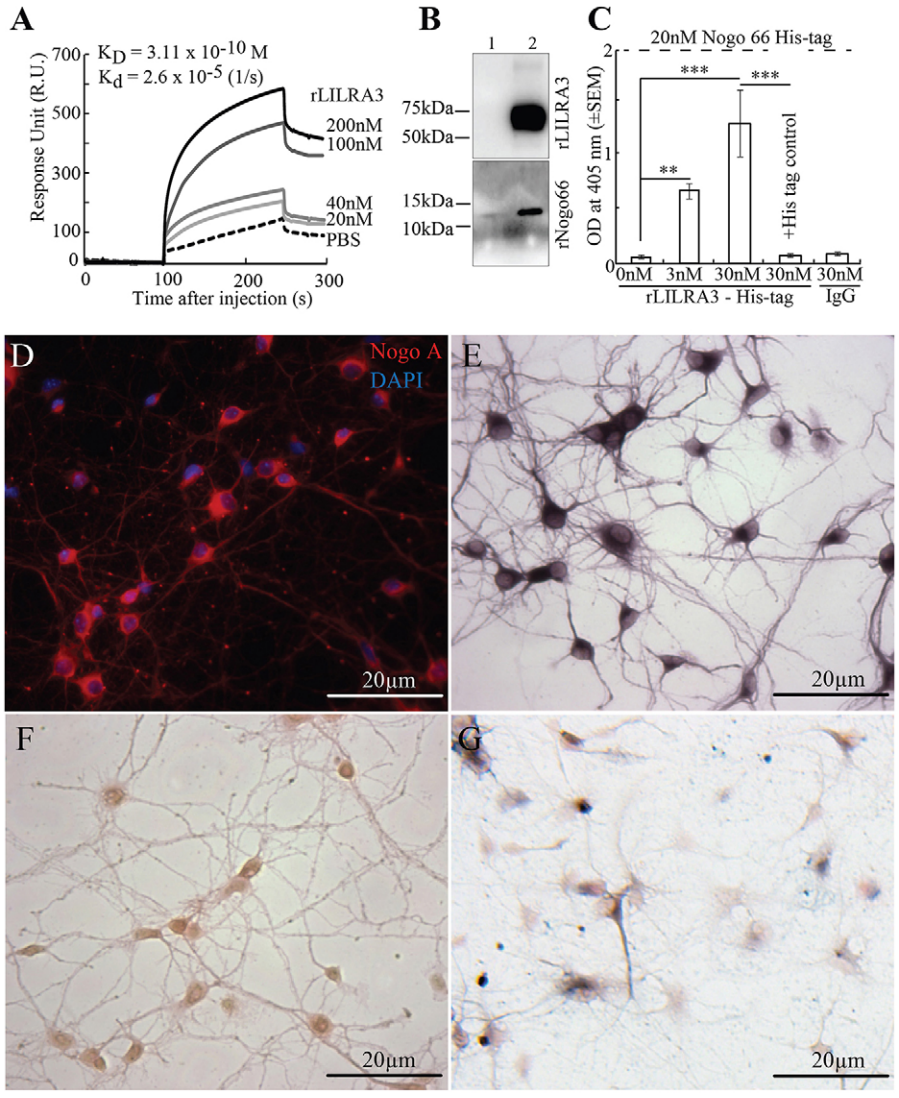

Fig. 1. Nogo 66 is a new high-affinity ligand for the LILRA3 receptor. (A) Representative SPR profiles of various concentrations of LILRA3 binding to chip-immobilised Nogo 66 [K_D=3.11×10^{-10} M; K_d (1/s)=2.6×10^{-5}] (n=3). (B) ConA–Sepharose-immobilised recombinant LILRA3–His (rLILRA3, lane 2) but not ConA–Sepharose alone (lane 1) precipitated recombinant Nogo 66, detected by western blotting using rabbit anti-Nogo antibody. Blotting of same membrane with anti-LILRA3 monoclonal antibody confirmed immobilisation of recombinant LILRA3 onto ConA–Sepharose (lane 2), whereas ConA–Sepharose alone did not immobilise LILRA3 (lane 1) (n=5 experiments). (C) His-tagged recombinant Nogo 66 bound plate-immobilised purified untagged recombinant LILRA3 in a concentration-dependent manner. His tag control protein did not bind the maximal concentration of plate-immobilised recombinant LILRA3, and Nogo 66 did not bind human IgG control confirming specificity. Results are mean± s.e.m. (n=4). **P<0.01, ***P<0.001 (one-way ANOVA). (D) Representative primary mouse cortical neurons cultured on PDL-coated coverslips for 4 days stained with rabbit anti-Nogo A antibody showing abundant expression of Nogo A in red (n=5). LILRA3–AP (E) but not control alkaline phosphatase tag (F) bound to the surface of these neurons *in situ* (blue staining, neutral red counterstain). (G) LILRA3–AP binding was markedly reduced by pre-incubation with 10 µg/ml rabbit antibody against Nogo A and Nogo B for 30 min, confirming specificity (n=4).

Journal of Cell Science (2016) 129, 1198-1209 doi:10.1242/jcs.182006

(Fig. 1B). Third, recombinant Nogo 66 bound to LILRA3, but not relevant negative controls, in a concentration-dependent manner (Fig. 1C). Fourth, mammalian-produced, optimally glycosylated soluble LILRA3 (Lee et al., 2013) bound native Nogo A on the surface of cultured primary cortical neurons with high affinity (Fig. 1D–F) and pre-incubation of neurons with anti-Nogo A antibody markedly blocked *in situ* LILRA3 binding (Fig. 1G), indicating specific binding (n=4). This was confirmed using live cortical neurons, which bound LILRA3–AP protein but not alkaline phosphatase showing specific binding (Fig. 2A; n=6, P<0.001). Importantly, binding of LILRA3–AP to these neurons was high affinity, saturable and yielded a straight line Scatchard plot (Fig. 2B,C). The apparent dissociation constant of interaction was, K_d=6.70×10^{-8} M and maximum specific binding (B_{max}) of 0.154×10^{-8} M. Nogo A gene silencing using specific short hairpin RNA (shRNA) on primary cortical neurons significantly reduced Nogo A mRNA (Fig. 2D) and protein (Fig. 2E) by ∼70% and 55% respectively, leading to a significant 34.3±8.6% (mean±s.e.m.) reduction in binding to LILRA3–AP compared to neurons transfected with scrambled shRNA (Fig. 2F; n=3, P<0.05). These results were consistent with *in situ* anti-Nogo antibody blocking experiments (Fig. 1G), and strongly corroborated the SPR and co-immunoprecipitation studies.

LILRA3 significantly reversed Nogo-66-mediated inhibition of neurite outgrowth in mouse and human cortical neurons

Ligation of the inhibitory receptor PIRB/LILRB2 and NgR1 on neurons by Nogo 66 leads to inhibition of neurite outgrowth (GrandPré et al., 2000; Schwab, 2010). In Fig. 3A, we show a schematic where competitive binding of soluble LILRA3 with Nogo 66 reverses the inhibitory effects of Nogo 66 binding to the closely related inhibitory cell surface receptors PIRB and LILRB2. To address whether this occurs, we established an *in vitro* neurite outgrowth inhibition model by culturing primary mouse cortical neurons that constitutively express surface PIRB (Fig. 3B,C) on plate-immobilised recombinant Nogo 66, and assessed potential competitive effects of recombinant LILRA3. As expected, the neurite length of neurons plated on recombinant Nogo-66–His-coated coverslips were significantly shorter (170.7±73 µm; Fig. 4A,H) than neurons cultured on control His-tag peptide control-coated coverslips (593.3±37 µm) (Fig. 4E,H; mean±s.e.m.; n=7, P<0.001). Importantly, Nogo-66-mediated inhibition of neurite outgrowth was dramatically reversed by co-incubation with recombinant LILRA3; the average length of 773.9±38 µm was five times longer than neurons cultured on recombinant Nogo 66 (Fig. 4C,H; n=7, P<0.001). Consistent with these results, staining for βIII tubulin (a neuron-specific marker) and Tau1 (also known as microtuble-associated protein tau; a marker for axonal development) in neurons cultured on Nogo 66 was limited and patchy, likely due to a poorly developed neuronal network (Fig. 4B). In contrast, neurons cultured on recombinant Nogo 66 with recombinant LILRA3-coated coverslips retained extensive staining for both proteins (Fig. 4D), indicating that LILRA3 reversed inhibition of neurite and axonal growth outgrowth by Nogo 66 and promoted substantial dendrite and axonal development. Interestingly, neurons cultured on recombinant

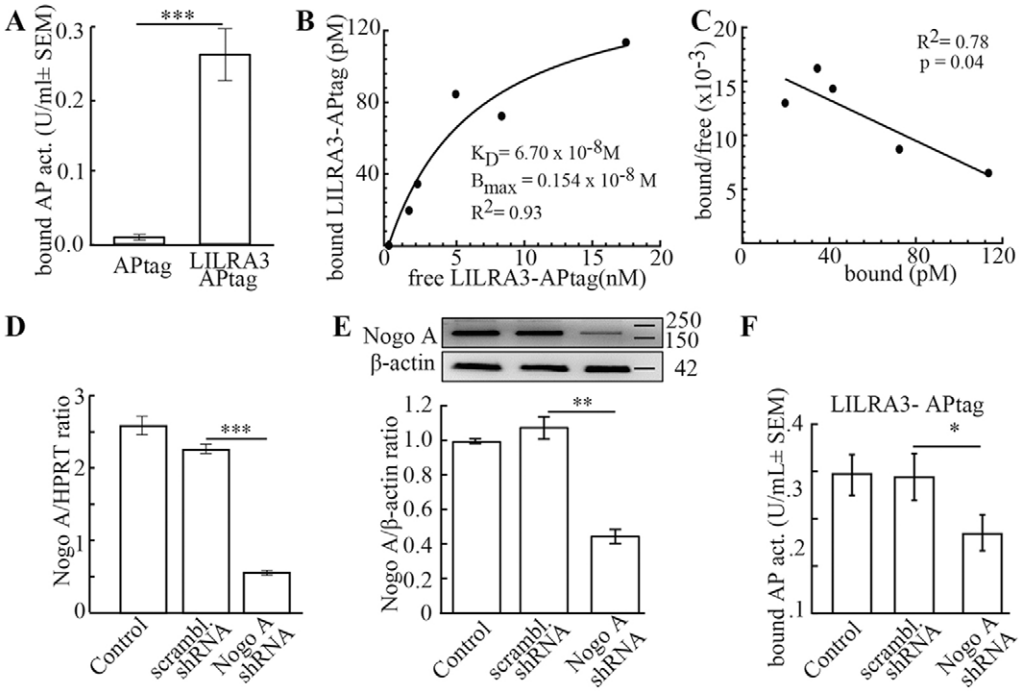

Fig. 2. High-affinity interaction of recombinant LILRA3 to cell surface Nogo on primary mouse cortical neurons. (A) Significant binding of LILRA3–AP but not alkaline phosphatase tag control to the surface of cortical neurons. Results are mean±s.e.m. (n=6). ***P<0.001 (one-way ANOVA). (B) Representative Scatchard analysis of LILRA3–AP binding to primary cortical neurons showing saturable high-affinity binding (K_d=6.70×10^{-8} M, B_{max}=0.154×10^{-8} M, R^2=0.93) (n=3). (C) Data in B presented as a Scatchard plot yielded a straight line plot, typical of a saturable receptor–ligand interaction (P=0.04, R^2=0.78). (D) Transient 5-day knockdown in primary cortical neurons using lentivirus-based shRNA reduced Nogo A mRNA by 78.3±6.3% (mean±s.e.m.) compared to neurons transfected with scrambled shRNA (n=3). ***P<0.001 (one-way ANOVA). (E) Representative western blot using antibody against Nogo A and Nogo B showing decreased levels of Nogo A protein (identified by its molecular mass of ∼180 kDa) in transfected cells (upper panel) and a summary densitometry (lower panel) of three independent western blot experiments showing 55.1±8.2% (mean±s.e.m.) reduction in Nogo A protein after specific gene silencing as compared to scrambled shRNA. **P<0.01; one-way ANOVA). (F) Nogo A shRNA gene silencing in primary cortical neurons significantly abrogated surface binding of LILRA3–AP by 34.3±8.6% (mean±s.e.m.) compared to neurons treated with scrambled shRNA (n=3). *P<0.05 (one-way ANOVA).

Journal of Cell Science

Journal of Cell Science (2016) 129, 1198-1209 doi:10.1242/jcs.182006

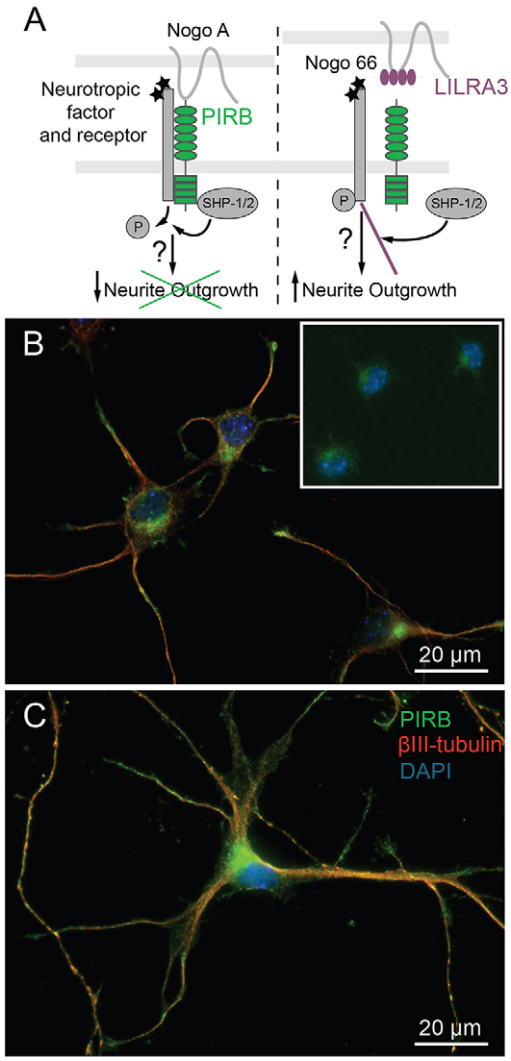

Fig. 3. Schematic representation of Nogo-66-mediated inhibition of neurite outgrowth. (A) Proposed diagram of the interaction between the 66-amino-acid loop of Nogo A with PIRB-transducing inhibitory signals in neurons, leading to inhibition of neurite outgrowth (left); soluble LILRA3 might competitively bind Nogo 66 and block its interaction with PIRB leading to reversal of neurite growth inhibition (right). (B,C) Representative immunofluorescence staining showing PIRB (green) expression on the surface of βIII-tubulin-positive (red) mouse cortical neurons cultured for 3 days and 7 days, respectively (n=10); similar results were observed in freshly isolated neurons (inset in B). These neurons were used for *in vitro* functional studies using plate-immobilised recombinant Nogo 66 with or without recombinant LILRA3.

LILRA3-coated coverslips were 15–25% longer than those with His tag alone (Fig. 4G,H, P<0.05), suggesting that LILRA3 might also have partially reversed negative effects caused by native Nogo A expressed on these neurons (Fig. 1D).

To confirm that LILRA3 modulated Nogo-66-induced inhibition of neurite outgrowth in human neurons, LILRB2-expressing primary human fetal cortical neurons were cultured on Matrigel-coated plates with or without recombinant Nogo 66 and with or without recombinant LILRA3 for 8 days. As expected, Nogo 66 inhibited neurite outgrowth (average length 270.4±85.3 µm) (Fig. 5A,E) compared to the His tag control (average length of 466.3±50.7 µm) (Fig. 5C,E; mean±s.e.m.; n=4, P<0.01). Importantly, co-treatment with recombinant LILRA3 significantly reversed Nogo-66-mediated inhibition, yielding neurite lengths of 530.2±36.7 µm (Fig. 5B,E; P<0.01). This length was twice that of neurons grown on Nogo 66-coated plates and 1.3 times that of neurons on the His tag control (Fig. 5E). Furthermore, neurites of neurons grown on recombinant LILRA3 tended to be somewhat longer (544.8±110.1 µm) than those on the His tag control (Fig. 5E). This is the first demonstration that LILRA3 regulates neurite outgrowth in human and mouse cortical neurons through interaction with the highly homologous Nogo 66.

LILRA3 increased numbers of synaptic contacts in mouse cortical neurons

Mouse cortical neurons cultured on coverslips coated with recombinant Nogo 66 for 21 days had an average of 135.6±12.0 synaptophysin and PSD95 (also known as DLG4) double-positive spots (i.e. synaptic contacts) per field of view (77.5×77.5 µm area) (Fig. 6A–C,J). This number was significantly less than the number of synaptic contacts of neurons cultured on His tag control coverslips (324.4±9.6 per field; Fig. 6G–I,J; median±s.e.m., n=3, P<0.0001). Importantly, co-coating with recombinant LILRA3 completely reversed recombinant Nogo 66-mediated inhibition and increased synaptic contacts to 337.6±7.8 per field, numbers similar to those in control neurons (Fig. 6D–F,J). Similarly, staining of neurons cultured for 14 days with synaptophysin and phalloidin, as pre-and post-synaptic markers, respectively, showed significantly less synaptic contacts in neurons grown on Nogo-66-coated coverslips as compared to those with Nogo 66 plus LILRA3 (Fig. S2).

LILRA3 reverses Nogo-66-mediated de-phosphorylation of ERK and MEK

Mouse cortical neurons cultured in growth-promoting neurobasal medium containing B-27 supplement were cultured for 1 h with recombinant Nogo 66 with or without recombinant LILRA3, and phosphorylation of potentially relevant kinases was assessed (Maeda et al., 1999; Nash et al., 2009). Neurons cultured on Nogo-66-coated dishes showed marked suppression of extracellular signal regulated kinases 1 and 2 (ERK1/2, also known as MAPK3 and MAPK1) and mitogen-activated protein tyrosine kinase kinase 1 and 2 (MEK1/2, also known as MAP2K1 and MAP2K2) phosphorylation compared to neurons cultured on control His-tag-coated dishes (Fig. 7; n=2). Importantly, Nogo-66-mediated suppression ERK1/2 and MEK1/2 phosphorylation was completely reversed by co-culture with LILRA3 (Fig. 7). There was slight suppression of p38 MAPK phosphorylation in response to Nogo 66, that was also reversed by LILRA3, whereas AKT phosphorylation was minimally affected by any combination of Nogo 66 with or without recombinant LILRA3 (Fig. 7).

DISCUSSION

Clinical association studies (Koch et al., 2005; Kabalak et al., 2009; Ordóñez et al., 2009; An et al., 2010; Du et al., 2014) and limited *in vitro* experiments (Lee et al., 2013) suggest that soluble LILRA3 might have immune regulatory roles in chronic inflammation but its exact functions are unclear, primarily due to insufficient knowledge of its natural ligands. Here, we used mammalian-produced recombinant LILRA3, with a structure typical of the native protein (Lee et al., 2013), as bait, and reproducibly identified three binding proteins with high MASCOT scores using mass peptide sequencing. These corresponded to Nogo 66, 67-kDa laminin receptor and HLA-B. Identification of the MHC class I protein confirmed earlier findings showing that LILRA3 bound to

Journal of Cell Science (2016) 129, 1198-1209 doi:10.1242/jcs.182006

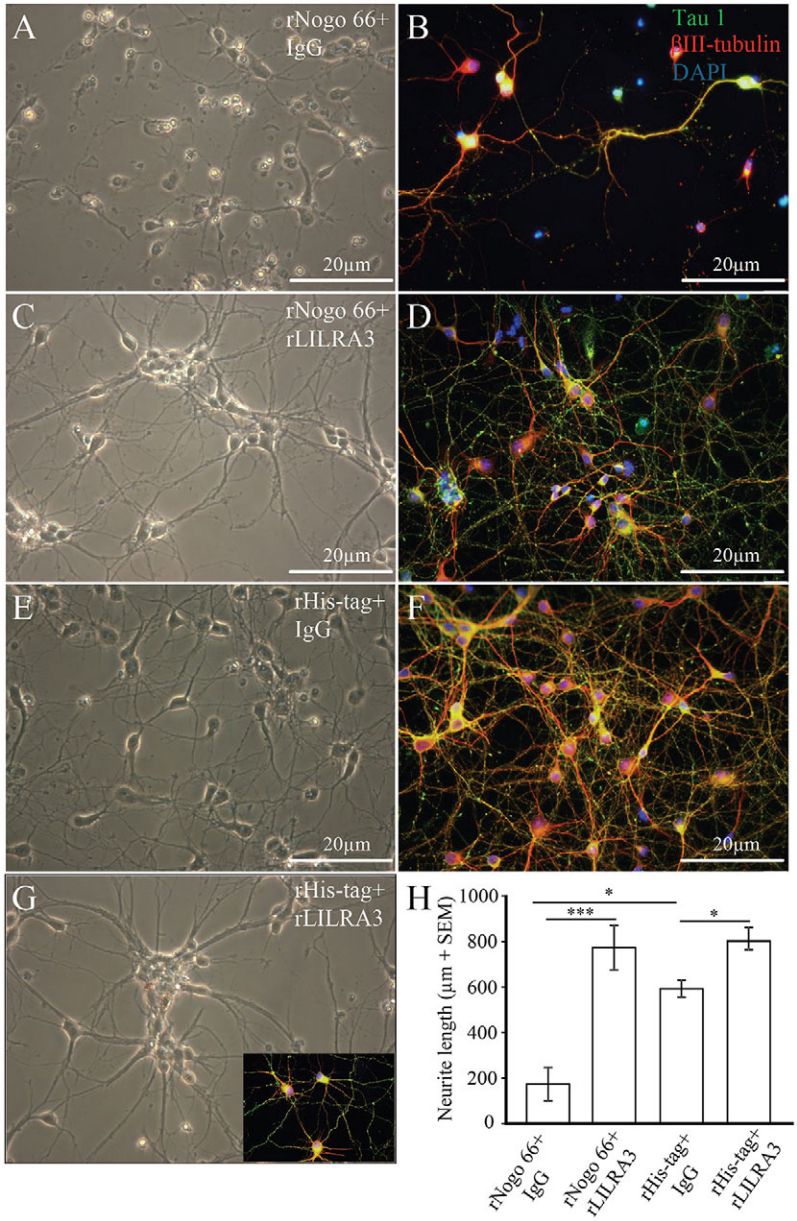

Fig. 4. LILRA3 significantly reversed Nogo-66-mediated inhibition of neurite outgrowth in mouse cortical neurons. (A,B) Representative images of primary mouse cortical neurons cultured for 4 days on PDL-coated coverslips that were spotted with recombinant Nogo 66 showing little scattered neurite outgrowth (A) and sporadic βIII tubulin (red) and Tau1 immunoreactivity (green) (B). (C,D) Images showing complete reversal of Nogo-66-mediated inhibition of neurite outgrowth (C) and enhanced β-III tubulin and Tau1 staining (D) in neurons co-incubated with recombinant LILRA3. (E,F) Neurons cultured on coverslips coated with control recombinant His (rHis-tag) and human IgG. (G) Neurons cultured on recombinant LILRA3-coated coverslips in the presence of control recombinant His tag but absence of Nogo 66 show promoted neurite outgrowth, and enhanced βIII tubulin and Tau1 expression (inset). (H) Summary of neurite length of randomly selected neurons; lengths of 30 neurons were measured per treatment per experiment (n=7) and presented as mean±s.e.m. *P<0.05, ***P<0.001 (one-way ANOVA). All phase-contrast images were acquired using a 40× objective and fluorescent images were acquired using a 63× objective.

single HLA-B- or HLA-C-coated beads (Jones et al., 2011). However, this is the first report to show concomitant binding of LILRA3 to an MHC-class I and two new non-MHC ligands, raising the possibility of multiple ligands of varying affinities. Consistent with this, the closely related cell surface receptor, LILRB2 has been shown to functionally interact with various MHC class I proteins (Cosman et al., 1997; Colonna et al., 1998; Shiroishi et al., 2003) and non-MHC ligands with varying affinities including interaction with angiopoietin-like proteins (Zheng et al., 2012) and β-amyloid (Kim et al., 2013). Of particular interest in our study was the high-affinity interaction of LILRA3 with Nogo 66, suggesting that LILRA3 might have new functions in the CNS, distinct from its expected immunoregulatory roles in leukocytes (Lee et al., 2013). We rigorously validated this interaction using several independent methods, including SPR, biochemical and immunochemical techniques (also see Fig. S4). Extensive ligand–binding studies showed that LILRA3 specifically bound to primary mouse cortical neurons with high affinity, and binding was saturable and specific. We confirmed that these neurons expressed high levels of Nogo A, and successful abrogation of binding by anti-Nogo antibody and following Nogo A gene silencing validated that LILRA3 binding was in the most part mediated by Nogo A. Interestingly, LILRB2, which has 82% sequence identity to LILRA3 (Borges and Cosman, 2000), and mouse PIRB also bind Nogo 66 (Atwal et al., 2008), suggesting a shared ligand.

Nogo 66 inhibits neurite outgrowth through interaction with PIRB (Atwal et al., 2008), although PIRB-mediated signalling events in neurons remain unclear. Based on our knowledge of PIRB-mediated inhibitory signalling pathways in leukocytes (Maeda et al., 1999), we propose that binding of Nogo 66 to PIRB might inhibit neurite outgrowth by de-phosphorylating growth-promoting protein tyrosine kinases (Figs 3A and 8A). Indeed, ERK1/2 and MEK1/2 phosphorylation in mouse cortical neurons cultured on recombinant Nogo-66-coated coverslips was profoundly suppressed and this was associated with reduced neurite outgrowth. Importantly, recombinant LILRA3 markedly reversed Nogo-66-mediated suppression of ERK1/2 and MEK1/2 phosphorylation and promoted neurite outgrowth. Effects of Nogo

Journal of Cell Science

Journal of Cell Science (2016) 129, 1198-1209 doi:10.1242/jcs.182006

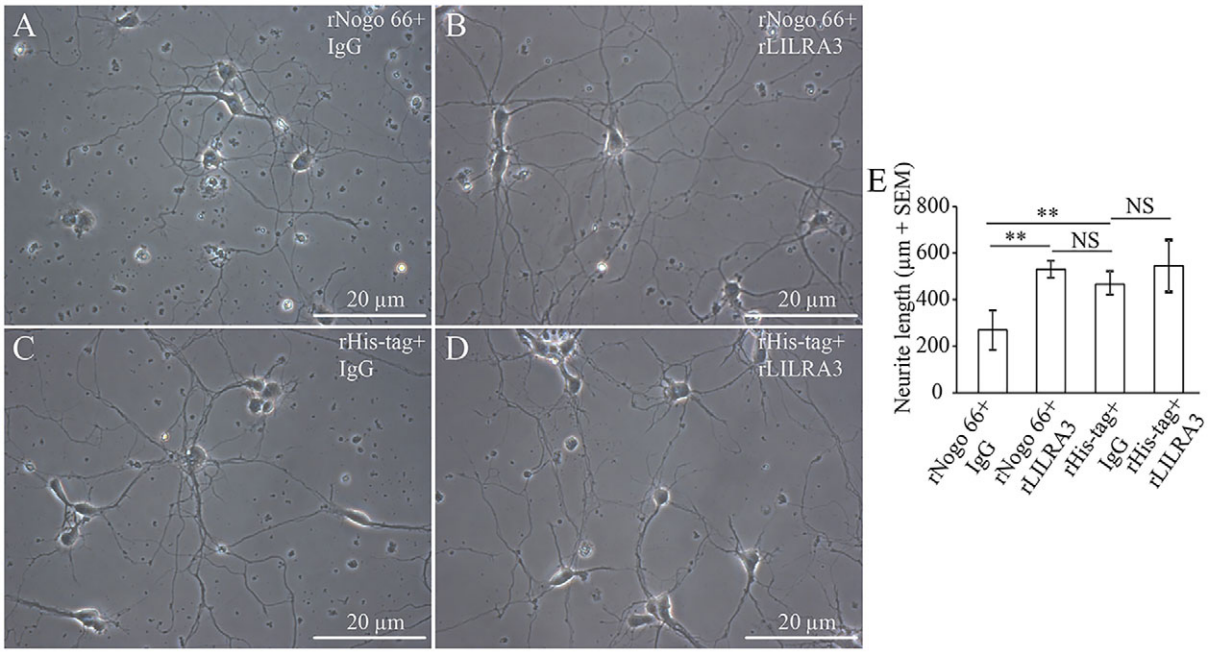

Fig. 5. LILRA3 significantly reversed Nogo-66-mediated inhibition of neurite outgrowth in human cortical neurons. (A) Representative primary human cortical neurons cultured for 8 days on PDL–matrigel-coated plates that had been spotted with recombinant (r)Nogo 66 showing diminished neurite outgrowth. (B) Significant reversal of Nogo-66-mediated inhibition of neurite outgrowth on plates co-coated with recombinant Nogo 66 and recombinant LILRA3. (C) Neurons cultured on coverslips coated with control recombinant His and human IgG. (D) Neurons cultured on recombinant-LILRA3-coated plates in the absence of recombinant Nogo 66 had similar neurite lengths compared to control IgG-coated plates (C), suggesting no tropic effects with LILRA3 alone. (E) Summary of neurite length measurement on 20 randomly selected neurons per treatment per experiment. Data are mean±s.e.m. of four independent experiments performed in duplicates. $^{**}P<0.01$; NS, not significant (one-way ANOVA). All images were acquired using a 40× objective.

66 on p38 MAPK phosphorylation were modest and there was little effect on AKT phosphorylation suggesting a more specific regulation of the ERK/MEK pathway. To our knowledge this is the first report showing Nogo-66-mediated suppression of ERK and MEK phosphorylation in primary neurons that was successfully reversed by LILRA3. Although further investigation is required, we speculate that suppression of ERK and MEK phosphorylation in Nogo-66-treated neurons occurs through its ligation of PIRB, which in turn promotes recruitment of SH2-domain-containing protein tyrosine phosphatases (SHP-1 and/or SHP-2, also known as PTPN6 and PTPN11, respectively) thereby deactivating signalling and causing neuronal growth arrest (Fig. 8A). Consistent with this, ligation of PIRB on the surface of neurons restrictes plasticity in the visual cortex (Syken et al., 2006) and suppresses axonal regeneration (Fujita et al., 2011a) through recruitment of SHP-1 and/or SHP-2, and limited data indicates that the recruited SHP-1 and/or SHP dephosphorylate (deactivate) tropomyosin receptor kinase B (TrkB, also known as NTRK2) leading to suppression of downstream MAPK signalling (Nash et al., 2009).

In addition to PIRB, Nogo 66 can inhibit neurite outgrowth by interacting with NgR1 that forms a complex with transmembrane proteins LINGO1, and p75 (also known as NGFR) or TROY (also known as TNFRSF19) to increase intracellular Ca^{2+} and activate the small GTPase RhoA and its effector protein Rho-associated, coiled-coil containing protein kinase 1 (ROCK1) eventually leading to growth arrest (Fournier et al., 2003; Nash et al., 2009; Schwab, 2010). LILRA3-mediated reversal of neurite growth might also in part be due to competitive blocking of the Nogo-66–NgR1 interaction by soluble LILRA3 thereby regulating this pathway (Fig. 8A,C), although this requires further research. Interestingly, p75 enhances the ability of PIRB to recruit SHP-1 and SHP-2 (Fujita et al., 2011b), suggesting a cross-talk between the NgR1 and PIRB signalling pathways.

The reversal of Nogo-66-mediated inhibition of neurite outgrowth by LILRA3 was similar in human and mouse cortical neurons, strongly validating our finding. It is possible that LILRA3 exerts positive effects in human neurons by competitively blocking the LILRB2–Nogo-66 interaction, although this requires further investigation. Importantly, this study is the first to demonstrate a human LILR protein having cross-species functions in mice and man, despite lack of LILRs in rodents, likely due to the high similarity of the shared Nogo 66 ligand. This property would allow more thorough investigation of LILR functions using an unlimited source of cultured primary mouse neurons, and opens for the first time opportunities to explore *in vivo* LILR functions, such as the use of tissue-specific transgenic expression of human LILRA3 in rodents, to investigate its role in the CNS.

Here, we provide evidence that LILRA3 as a new high-affinity soluble receptor consistently and significantly reversed Nogo-66-mediated inhibition of neurite outgrowth and synapse formation *in vitro* by 60–70%. These effects are comparable to or better than other known inhibitors, including antibodies against Nogo A, Nogo A gene deletion, the use of soluble NgR fragments, NgR-blocking peptides, inhibitors of Rho-A and ROCK or inhibitors of intracellular Ca^{2+} influx (Schwab, 2004). Importantly, unlike these inhibitors, LILRA3 is an endogenous protein making it an attractive therapeutic candidate. We propose that LILRA3 might act as a broad-spectrum competitive antagonist to a range of inhibitory Nogo receptors including PIRB/LILRB2 and NgR1 (Fig. 8A–C). Although methodological differences should be accounted for and future concurrent comparative studies are required, our SPR results indicate that the binding affinity of Nogo 66 to LILRA3 is 10–100

Journal of Cell Science

Journal of Cell Science (2016) 129, 1198-1209 doi:10.1242/jcs.182006

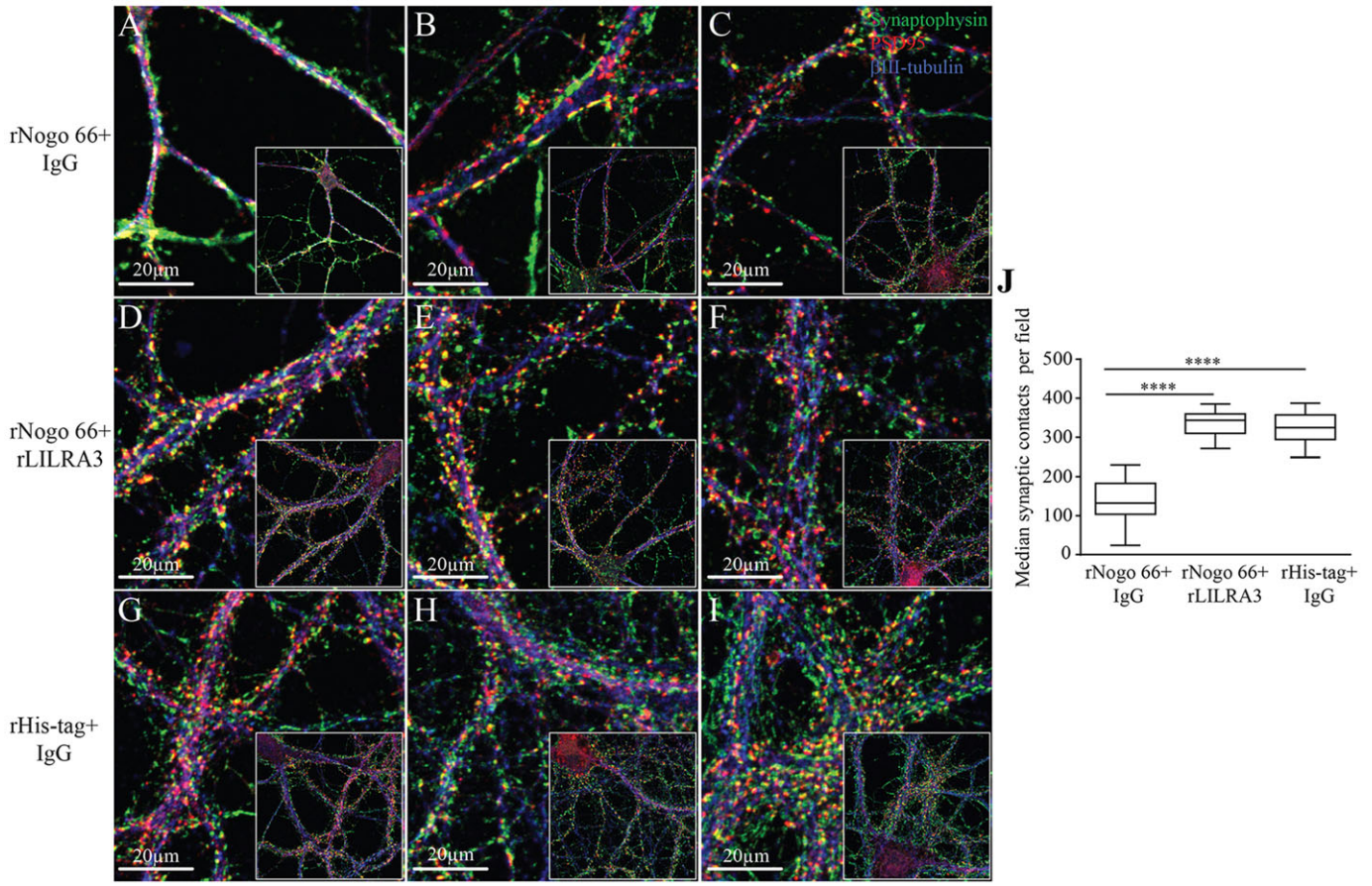

Fig. 6. LILRA3 increased density of synaptic contacts in mouse cortical neurons cultured for 21 days. (A–C) Representative images of three independent primary mouse cortical neurons cultures on PDL-coated coverslips that were spotted with recombinant (r)Nogo 66 plus control IgG had reduced numbers of synaptic contacts, as demonstrated by a decreased number of spots staining for both synaptophysin (green) and PSD95 (red); βIII tubulin was used as marker for dendrites (purple). (D–F) Co-incubation of neurons with recombinant LILRA3 reversed the Nogo-66-mediated inhibition resulting in increased numbers of synaptic contacts to numbers, comparable to His tag control neurons (G–I). (J) Box-whisker plots of synaptic contacts of three independent neurons cultures under the different treatment conditions showing significantly lower synaptic contacts for neurons cultured on coverslips spotted with Nogo 66 plus IgG (median=132 contacts) as compared to neurons grown on Nogo 66 plus LILRA3 (343.6 contacts) or control His-tag-coated coverslips (324.5 contacts). ****P<0.0001 (one-way ANOVA). The box represents the 25–75th percentiles, and the median is indicated. The whiskers show the complete range.

times higher than its binding to PIRB (Matsushita et al., 2011) or NgR1 (Lauren et al., 2007). These properties are consistent with a typical soluble competitive antagonist with broad functional specificity. Interestingly, we found constitutive expression of LILRA3 in neurons derived from fetal cortical brain and in normal adult brain tissue, suggesting physiological functions (Fig. S3). Future studies that systematically map expression patterns and identify cellular sources of LILRA3 and define its relationships to Nogo A in the brain during health and disease could provide new insights into its pathophysiological roles in the CNS.

MATERIALS AND METHODS

Production of recombinant proteins

C-terminal placental alkaline-phosphatase-tagged (LILRA3–AP), 6xHis-tagged (LILRA3–His) and untagged high-quality full-length LILRA3 recombinant proteins were produced in 293T HEK cells as described previously (Lee et al., 2013). Large-scale therapeutic grade LILRA3–His recombinant protein in PBS was custom-made in 293FT HEK cells in collaboration with the Commonwealth Scientific and Industrial Research Organisation (CSIRO, VIC, Australia). Purified human IgG_1 was purchased from Jackson ImmunoResearch (PA, USA) and used as negative control to LILRA3. Human C-terminal 6xHis-tagged Nogo 66 (Nogo-66–His) was subcloned from Nogo 66 in pGEX2 (Pei-hua Lu, Shanghai University, China) into pET30 EK/LIC (Novagen, Darmstadt, Germany) using forward primer 5′-GACGACGACAAGATGAGGATATACAAGGGT-3′ and reverse primer 5′-GAGGAGAAGCCCGGTTCACTTCAGAGAATC-3′ and protein was expressed in BL21 DES *E. coli* cells. Soluble recombinant Nogo-66–His protein was purified using fast protein liquid chromatography (FPLC, BioLogic DuoFlow, Bio-Rad, NSW, Australia) and reverse-phase high-pressure liquid chromatography 600S HPLC (Waters Corporation, MA, USA) on a C8 column (Sigma, MO, USA). Aliquots of purified Nogo-66–His were resuspended in water (1 mg/ml), tested for lipopolysaccharide (LPS) and used within 1 week. 6xHis-tag peptide in pET30 EK/LIC was expressed BL21 DES *E. coli* cells, purified as above and used as the relevant control.

Identification of LILRA3-binding proteins from peripheral blood mononuclear cells by mass spectrometry

Peripheral blood mononuclear cells (PBMCs) from healthy donors were lysed in a non-detergent lysis buffer using N_2-cavitation (Hartgroves et al., 2003). In brief, 10^8 PBMCs were washed once in H-buffer (10 mM HEPES pH 7.2, 250 mM sucrose, 2 mM $MgCl_2$, 10 mM NaF and 1 mM vanadate) and suspended in 3 ml H-buffer containing protease inhibitor cocktail (Roche, Australia), then dissociated using a Nitrogen cavitation chamber at 50 bar, 4°C for 10 min (Parr Instrument Company, IL, USA). Plasma membrane from cell homogenates was separated by sucrose gradient ultracentrifugation (Gaus et al., 2001). Protein concentrations were adjusted

Journal of Cell Science (2016) 129, 1198-1209 doi:10.1242/jcs.182006

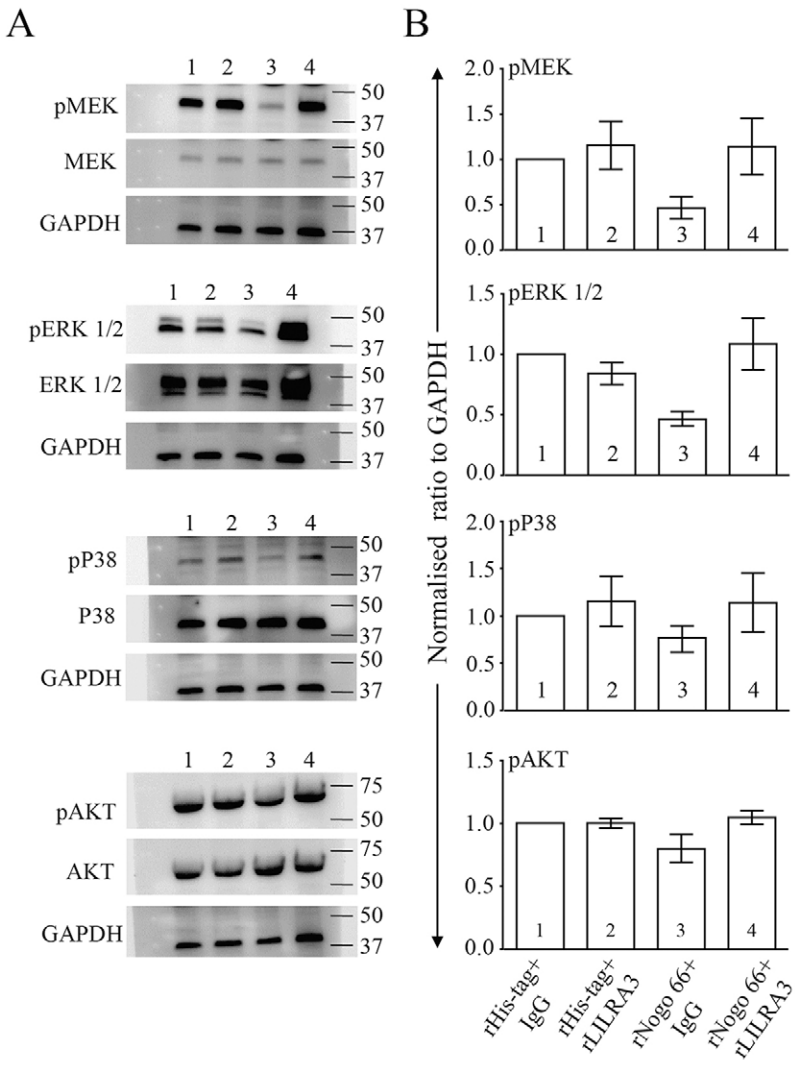

Fig. 7. Regulation of the ERK/MEK signalling pathway by recombinant LILRA3 and Nogo-66-mediated inhibition of neurite outgrowth. (A) Mouse cortical neuron plated onto coverslips coated with recombinant (r)His tag control and a control protein (human IgG) (1) or recombinant His tag and recombinant LILRA3 (2) for 1 h showed phosphorylation (p) of MEK and ERK1/2 that was markedly reduced on neurons cultured on coverslips coated with recombinant Nogo 66 and human IgG (3). Nogo-66-mediated dephosphorylation of ERK1/2 and MEK was completely reversed in neurons cultured on coverslips coated with recombinant Nogo 66 and recombinant LILRA3 (4). Phosphorylation of p38 MAPK was marginally altered by recombinant Nogo 66 and/or recombinant LILRA3 and there was no effect on AKT. (B) Summary densitometry of two independent experiments showing marked suppression of ERK1/2 and MEK phosphorylation by recombinant Nogo 66, which was completely reversed by recombinant LILRA3.

to 5 mg/ml in HBHA ligand-binding buffer (HBSS plus 0.5 mg/ml BSA, 0.1% NaN_3, 20 mM HEPES and protease inhibitors, pH 7.0). 500 µl (2.5 mg) membrane protein was incubated with 500 nM LILRA3–AP (experimental) or alkaline phosphatase (control) protein for 90 min at room temperature, and LILRA3–AP bait was co-immunoprecipitated with LILRA3-binding proteins by incubating samples with 20 µg (20 µl) Sepharose-conjugated anti-placental alkaline phosphatase monoclonal antibody (catalogue number Q332, GenHunter, TN) for 2 h at 4°C. Sepharose-bound proteins were precipitated by centrifugation and washed twice with Tris buffer (10 mM Tris-HCl, pH 8, 140 mM NaCl and 0.025% NaN_3) containing 0.1% Triton X-100 and 0.1% bovine haemoglobin (Sigma, NSW, Australia), followed by 4 washes with Tris buffer and a final wash with 50 mM Tris-HCl, pH 6.8. Sepharose bead pellets from experimental and control samples were resuspended in 30 µl SDS-PAGE gel loading buffer containing 10 mM DTT, boiled at 100°C for 5 min and loaded onto a 10% one-dimensional SDS-PAGE gel and run under reducing conditions. Gels were washed three times with Tris-buffered saline (TBS) then silver stained, and excised bands sent to the Bioanalytical Mass Spectrometry Facility at University of New South Wales for tryptic digest and peptide mass sequencing using Nano LC-MS/MS. Comparisons of experimental and theoretical tandem mass spectra were automatically performed by Mascot version 2.0 (http://www.matrixscience.com), which scored peptide matches and correlated with protein identifications against *Homo sapiens* proteins in the Swissprot database. Precursor tolerances were 4.0 ppm and product ion tolerances±0.4 Da; acceptable cut-off scores for individual MS/MS spectra were set to 20 (Lee et al., 2013).

Surface plasmon resonance

SPR experiments were performed using a BIAcore 2000 (BIAcore, Uppsala, Sweden) to determine the equilibrium dissociation constant (K_d) between Nogo 66 and LILRA3. Briefly, negatively charged recombinant Nogo 66 was 'physisorbed' onto a research-grade positively charged untreated gold surface sensor chip (Sensor Chip AU, GE Healthcare, NSW, Australia) by a hydrophobic interaction at a flow rate of 5 µl/min to 500–600 response units (RU) as described previously (Melrose et al., 2006). After blocking sensor chips with BSA at a flow rate of 20 µl/min, chips were equilibrated in running buffer (PBS). Serially diluted recombinant LILRA3–His (20–200 nM) in PBS was injected over the immobilised flow cells at a rate of 20 µl/min for 3 min at 25°C. Binding responses with various concentrations were subtracted from the nonspecific responses to an empty flow cell. Kinetic constants were calculated with the BIA evaluation program (version 3.0.2; BIAcore).

Co-immunoprecipitation of Nogo 66 with LILRA3

Recombinant LILRA3–His (10 µg in 100 µl PBS) was immobilised onto 50 µl ConA-conjugated Sepharose (ConA, GE Healthcare, NSW, Australia) at 4°C overnight. After removing unbound protein by gentle centrifugation (200 ***g*** for 5 min at 4°C), beads were washed five times with cold 20 mM Tris-HCl, 150 mM NaCl, pH 7.4, and resuspended in 50 µl cold HBHA buffer. Recombinant Nogo-66–His (1 µg in 100 µl water) was then added to the bead slurry with or without immobilised LILRA3 and incubated for 2 h at 4°C. Unbound protein was then removed by centrifugation (800 ***g*** for 5 min at 4°C), and beads washed four times with Tris buffer and once with

Journal of Cell Science

Journal of Cell Science (2016) 129, 1198-1209 doi:10.1242/jcs.182006

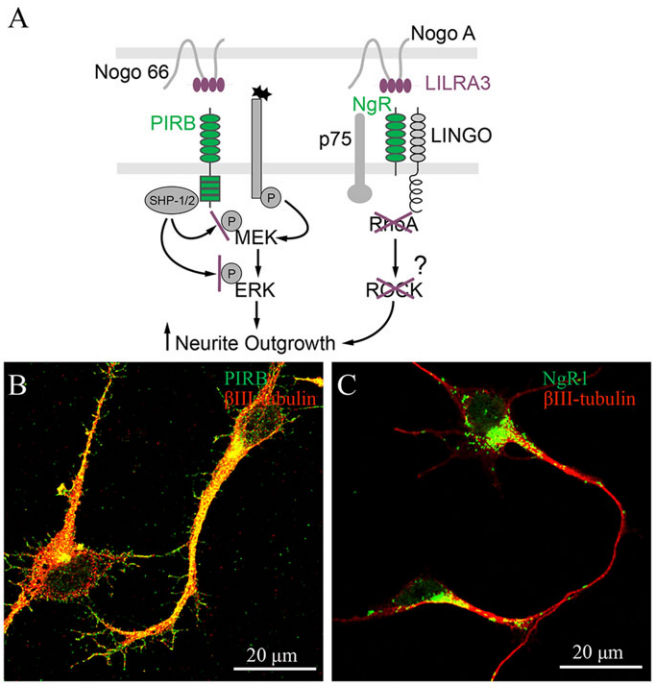

Fig. 8. Summary of the proposed mechanisms of LILRA3-mediated promotion of neurite outgrowth and synapse formation. (A) Soluble LILRA3 might block ligation of PIRB by Nogo 66 thereby preventing SHP-1 and/or SHP-2-mediated inhibitory signals by dephosphorylating (deactivating) key growth-promoting protein tyrosine kinases (left); similarly, LILRA3 might prevent ligation of NgR1 complex by Nogo 66 and the subsequent transduction of inhibitory signals (right). LILRA3 might therefore act as a soluble antagonist of PIRB and/or NgR by competitively binding to Nogo 66. (B,C) Representative immunofluorescence staining showing that both NgR and PIRB (green) are expressed on the surface of βIII-tubulin-positive (red) mouse cortical neurons cultured for 3 days ($n \geq 6$). Images acquired in 1024×1024 pixel array using Leica TCS SP5cw STED microscope and a 100× HCX Plan Apo NA 1.4 objective (Mannheim, Germany).

50 mM Tris-HCl, pH 6.8. Samples were separated by 10% SDS-PAGE under reducing conditions, transferred onto PVDF membranes and blocked with 5% low-fat milk plus 2% BSA in TBS for 2 h. Membranes were then immunoblotted with a rabbit antibody that recognises Nogo A and Nogo B (IMG-5346A, 1.5 μg/ml, Imgenex, CA, USA) at 4°C overnight followed by four washes with TBS+0.1% Tween 20 (TBST) then incubated with horseradish peroxidase (HRP)-conjugated goat anti-rabbit antibody (172-1034, 1:5000 dilution; Bio-Rad, NSW, Australia) for 2 h at room temperature. After four washes with TBST, immunoreactive bands were detected using Western Lightening Plus chemiluminescent substrate (PerkinElmer, MA) and images were acquired with a ImageQuant™ LAS4000 (GE Healthcare Life Sciences). Membranes were then washed four times with TBST then reblotted with mouse anti-LILRA3 monoclonal antibody (1 μg/ml; Abnova, Taipei, Taiwan) 4°C overnight followed by HRP-conjugated goat anti-mouse antibody (1:10,000 dilution; Bio-Rad, NSW, Australia) for 2 h at room temperature, washed four times and immunoreactive bands detected as above.

Binding of Nogo 66 to plate-immobilised LILRA3

96-well flat bottom Nunc MaxiSorp ELISA plates were equilibrated with 100 μl 0.05 M carbonate-bicarbonate buffer, pH 9.6 for 30 min at room temperature, then coated with increasing concentrations (0–30 nM) of untagged recombinant LILRA3 or maximum amounts (30 nM) of human IgG control in 200 μl TBS and incubated overnight at 4°C. Unbound proteins were aspirated, wells washed once in TBS then 20 nM recombinant Nogo-66–His or 20 nM His tag control in 200 μl TBS was added, and plates incubated for 2 h at room temperature. After removing unbound protein, wells were blocked with 5% BSA in TBS containing 0.05% Tween-20 (TBST) for 30 min at room temperature, washed three times with 200 μl/well TBST, then 50 μl mouse anti-His monoclonal antibody (0.5 μg/ml; Novagen, CA) diluted in TBST plus 5% BSA was added to each well and incubated at 4°C overnight. Wells were washed three times with TBST, incubated at room temperature for 2 h with 50 μl biotinylated goat anti-mouse antibody (1 μg/ml; DAKO, Glostrup, Denmark) in TBS, then washed three times with TBST and incubated with 50 μl Streptavidin–HRP (1:200 dilution; R&D Systems, MN) in TBS for 20 min at room temperature in the dark. After four washes with TBST, 100 μl of TMB substrate was added and plates were incubated in the dark for 1 h at room temperature, the reaction was stopped with 50 μl 1 M H_2SO_4 and optical density at 450 nm and 540 nm was measured (SpectraMax Plus plate reader, Molecular Devices, CA, USA).

Primary mouse and human cortical neuron cultures

Primary mouse cortical neurons were derived *in vitro* as described by us previously (Fath et al., 2009). Briefly, E16.5 embryos were harvested from C57B6 mice and cerebral cortices carefully dissected, enzymatically digested and sequentially triturated using a wide an then a narrow fire-polished glass pipette. Dissociated neurons in Dulbecco's modified Eagle's medium (DMEM) with 10% FBS were then carefully seeded (10^5 cells) onto poly-D-lysine (PDL)-coated wells or 12-mm coverslips. After 2 h, the medium was changed to neurobasal medium supplemented with 2% B27 and 2 mM Glutamax (Life Technologies, VIC, Australia), incubated at 37°C in 5% CO_2 air. The University of New South Wales Animal Ethics Committee approved the use of mouse fetal brain to derive cortical neurons in culture (reference number 13/119A).

Human fetal brains were obtained from 14–19-week fetuses after therapeutic termination. The collection of fetal brain tissue to derive human cortical neurons in culture was approved by Macquarie University Human Ethics Committee (reference number 5201300330). Informed consent was obtained from all donors and the investigations were conducted according the principles expressed in the Declaration of Helsinki. Neurons were prepared and phenotyped according to our established protocol (Guillemin et al., 2005, 2007). Briefly, 1–2 g cortical brain tissue was washed in PBS with 2% antibiotics and antimycotics (Life Technologies, VIC, Australia) then dissociated using neural tissue dissociation kits (Miltenyl Biotec, NSW, Australia). Cells were filtered through 40 μm nylon mesh, centrifuged (350 ***g*** for 10 min, at room temperature) and resuspended in complete neurobasal medium containing 2% B27, 2 mM Glutamax, 50 mM HEPES, 200 IU/ml penicillin G, 200 μg/ml streptomycin sulfate, and 5 mM glucose (Life Technologies, VIC, Australia) at 2×10^5/ml, seeded onto PDL-treated Matrigel-coated (Life Technologies, VIC, Australia) 24-well plates or 12-mm coverslips and then incubated at 37°C in 5% CO_2 and 95% air.

The LIVE/DEAD® assay kit that detects live cells that convert non-fluorescent Calcein AM into green fluorescent dye (fluorescence emission 530 nm) and dead cells that uptake EthD-1 (fluorescence emission at 645 nm) routinely showed >90% live cultured human neurons and >95% live mouse cortical neurons (Molecular Probes, OR). Treatment of these neurons with recombinant LILRA3 and/or recombinant Nogo 66, His tag control or anti-Nogo blocking antibody did not affect viability.

Nogo A gene silencing

Four Nogo shRNA constructs targeting Nogo A and B, and one scrambled shRNA in psi-LVRU6MP lentiviral vector containing mCherry fluorescent tag were custom-made by GeneCopoeia (MD). Nogo shRNA sequences were designed based on GeneBank accession number NM_024226.3. High-titre shRNA containing lentiviruses were produced in 293FT as described (Life Technologies; VIC, Australia). Freshly prepared viral supernatants were used to infect 10^6 primary mouse cortical neurons in six-well PDL-coated plates. In brief, neurons were cultured for 24 h in 2 ml complete neurobasal medium and then infected with 0.25 ml virus [multiplicity of infection (MOI)=1]. At 5 days after infection, neurons were used for RNA isolation, protein extraction or binding assays. After initial screening of all four shRNA constructs for Nogo A and B mRNA knockdown, we found that the Nogo A and B shRNA construct with target sequence 5′-GGCGCAGATAGATCATTATCT-3′ achieved the maximum Nogo A and B gene silencing (>70%). Gene silencing was validated by quantitative real-time PCR (qRT-PCR) using Nogo A primer sets (forward

5′-CAGTGGATGAGACCCTTTTTGAT-3′ and reverse primers 5′-GCTGCTCCTTCAAATCCATAA-3′) and HPRT housekeeping gene (forward: 5′-AAGGACCTCTCGAAGTGTTGGATA-3′ and reverse primer: 5′-CATTTAAAAGGAACTGTTGACAACG-3′), and western blotting was performed with antibody against Nogo A and B (1.5 µg/ml, Imgenex, CA). Scrambled 5′-GCTTCGCGCCGTAGTCTTA-3′ shRNA and vector alone were used as controls.

Assessment of neurite outgrowth in cortical neurons

PDL-coated or PDL plus Matrigel-coated 24-well plates were first spotted with 2.5 µl (10 nM/spot) recombinant Nogo-66–His (total 48 spots/well) or His-tag control in duplicates and dried at 37°C for 1 h as described (GrandPré et al., 2000; Fournier et al., 2001). Wells were then rinsed with PBS and incubated overnight at 4°C with 150 µl recombinant LILRA3–His or human IgG in PBS (each 100 nM). Unbound proteins were aspirated; wells rinsed with 500 µl neurobasal medium and seeded with primary mouse or human cortical neurons at 5×10^4/well in 500 µl or 2×10^5/well in 1 ml complete neurobasal medium, respectively. Seeded mouse and human neurons were cultured at 37°C, in 5% CO_2 in air in a humidified incubator for 4 or 8 days, respectively, fixed with 4% paraformaldehyde in PBS for 10 min at room temperature, rinsed and resuspended in PBS. Contiguous phase-contrast digital images of the entire well at 20× and 40× objective were acquired using a Olympus CKX41 microscope mounted with Q Imaging 3.3 RTV camera and Olympus CellSens software version 1.8 (Olympus, VIC, Australia). The neurite lengths of randomly selected neurons in each well were then assessed by an independent observer using computer-assisted imaging (NIH-ImageJ2 software) as described previously (Curthoys et al., 2014). Neurite lengths of 30 neurons per treatment per experiment were measured for mouse neurons (n=7), and lengths of 20 neurons per condition in duplicates were measured for human neurons (n=4).

Binding of LILRA3–AP to mouse cortical neurons

In situ binding of LILRA3–AP or alkaline phosphatase control protein to mouse cortical neurons cultured on coverslips was assessed as described previously (Lee et al., 2013). For antibody-blocking, neurons on coverslips were pre-incubated for 30 min at room temperature with 10 µg/ml of the rabbit antibody against Nogo A and NogoB in HBHA without BSA, rinsed and incubated with LILRA3–AP or alkaline phosphatase control as described previously (Lee et al., 2013). Positive blue-stained neurons counterstained with 1% neutral red were visualised using an Olympus BX51 light microscope (Olympus, VIC, Australia). For quantitative binding studies, units of alkaline phosphatase activity were calculated from an alkaline phosphatase activity standard (Sigma, NSW, Australia) (Flanagan and Leder, 1990). For Scatchard analysis of binding, neurons were incubated with serially diluted LILRA3–AP (0–50 nM) and amounts of bound protein plotted against free protein or as ratios of bound to total protein (Flanagan and Leder, 1990).

Immunofluorescence staining

To compare effects on synapse formation, mouse cortical neurons were cultured for 21 days on PDL-coated 12-mm coverslips in four-well plates that were spotted (28 spots/coverslip; 10 nM/spot) with recombinant Nogo 66 with or without recombinant LILRA3–His with or without IgG control then were fixed with 4% paraformaldehyde in PBS for 10 min. After 10 min permeabilisation with 0.1% Triton X-100 in PBS and incubated overnight at 4°C with rabbit anti-synaptophysin mAb (2 µg/ml; Sapphire Bioscience, NSW, Australia) as a presynaptic marker and mouse-anti-PSD 95 (1 µg/ml; Chemicon, CA, USA) primary antibodies. This was followed by four washes and a 2-h incubation at room temperature with goat Alexa-Fluor-488-conjugated anti-rabbit-IgG and Alexa-Fluor-555-conjugated donkey anti-mouse-IgG antibodies (Molecular Probes, OR, USA) diluted in 0.1% Triton X-100 in PBS, respectively. Coverslips were then washed and incubated with chicken anti-β-III tubulin Ab (1.2 µg/ml; Millipore, VIC, Australia) for 2 h at room temperature. After four washes, coverslips were incubated with goat anti-chicken Alexa-Fluor-647-conjugated secondary antibody (1:500 dilutions; Molecular Probes, OR) for 2 h at room temperature, washed and wet mounted using ProLong® Gold Antifade reagent containing DAPI (Molecular Probes, OR). Images were acquired in 1024×1024 pixel array using a Leica TCS SP5cw STED microscope with a 100× HCX Plan Apo NA 1.4 objective (Mannheim, Germany). Numbers of synaptic contacts, defined as synaptophysin-positive pre-synaptic terminals (green) in direct contact with PSD95-positive post-synaptic protein (red) in 77.5×77.5 µm area (=1 field of view), were quantified using a custom-written MATLAB code (available on request). In brief, images from both channels were normalised to the maximum pixel value, before their intensity ratio was calculated to extract regions of the image with high colocalisation. In each channel, only pixels with values of two standard deviations above the average background were counted. Intensity ratio images were then processed identifying numbers of synapse contacts by two approaches, first using a spot detection and, second, using a water-shedding algorithm to segment and identify individual clusters (Klotzsch et al., 2015); both yielded similar results. Six randomly selected fields per sample per treatment in three independent experiments were measured.

Standard two-step immunofluorescence staining was used to determine effects of recombinant LILRA3 on axonal development and dendrite formation using mouse anti-Tau1 monoclonal antibody (MAB3420, 2 µg/ml; Millipore), and chicken anti-β-III tubulin, respectively (AB9354, 1.2 µg/ml; Millipore, VIC, Australia). Surface Nogo A, PIRB and NgR1 expression was determined using the rabbit antibody against Nogo A and Nogo B (IMG-5346A, 1.5 µg/ml; Imgenex, CA, USA), rat anti-PIRB monoclonal antibody (mAb, clone 326414, MAB2754, 0.5 µg/ml; R&D Systems) and rabbit-anti NgR1 antibody (AB15138, 5 µg/ml; Millipore, Australia), respectively. Fluorescent images were acquired using a 63× objective on Olympus BX51 microscope mounted with a DP73 camera and Olympus CellSens software version 1.8 (Olympus, VIC, Australia).

Western blot analysis of signalling molecules regulated in Nogo-66-mediated inhibition

Cortical neurons derived from E16.5 mouse embryos in neurobasal media supplemented with 2% B27 and 2 mM Glutamax were cultured for 1 h on PDL-coated 6-cm dishes spotted with recombinant Nogo-66–His and control IgG, recombinant LILRA3–His and control IgG, His-tag control and LILRA3 or His-tag control and control IgG as described above. Dishes were then rinsed with 3 ml PBS and lysed in 300 µl cell lysis buffer (150 mM NaCl, 50 mM Tris-HCl, 5 mM EDTA and 1% NP-40) containing 2 mg/ml protease inhibitors (Roche Applied Science) and 10 µM pervanadate (Sigma). Protein concentrations in cell lysates were determined using a BCA assay as described by the manufacturer (Thermo Scientific). Four sets of 20 µg cell lysate from each sample were separated by 10% SDS-PAGE under reducing conditions then transferred onto PVDF membranes. Membranes were blocked by 5% BSA in TBST (TBS with 0.1% Tween 20) for 2 h at room temperature then incubated with the primary rabbit antibodies against the following: anti-phosphorylated (p)-ERK1/2 [p-P44/42 MAPK (Erk 1/2) (Thr202/Tyr204), cat. no. 9101, 1:1000], anti-p-P38 MAPK (Thr180/Tyr182) (cat. no. 9215, clone 3D7, 1:1000), anti-p-MEK1/2 (Ser217/221) (cat. no. 9154, clone 41G9, 1:1000) or anti-p-AKT (Thr308) (cat. no. 2965, clone C31E5E, 1:1000) in TBST (Cell Signaling Technology, MA, USA) overnight at 4°C. Membranes were washed three times with TBST then incubated with goat HRP-conjugated anti-rabbit-IgG secondary antibody in TBST (Bio-Rad) for 2 h at room temperature, followed by three washes in TBST and immunoreactive bands detected using chemiluminescent substrate (Perkin Elmer). Images were acquired using ImageQuant™ LAS4000 on auto-setting (GE Healthcare Life Sciences). Membranes were then stripped using 62.5 mM Tris-HCl (pH 6.7), 100 mM β-mercaptoethanol (Sigma) in 2% SDS for 30 min at 50°C, rinsed thoroughly in TBS then blocked with the blocking buffer for 2 h room temperature. Total ERK, p38, MEK or AKT was detected using rabbit anti-total ERK1/2 [P44/42 (Erk1/2), cat. no. 9102, 1:1000], anti-total p38 MAPK (cat. no. 9212, 1:1000), anti-total MEK1/2 (cat. no. 9122, 1:1000) or anti-total AKT antibodies (cat. no. 9272, 1:1000) (Cell Signaling Technology) as above. GAPDH protein as a loading control was detected using rat anti-GAPDH monoclonal antibody

(Abcam, Cambridge, UK) followed by HRP-conjugated goat anti-rat antibody (Bio-Rad). Protein levels were semi-quantified using ImageJ densitometry analysis of samples relative to the corresponding GAPDH and then normalised to control samples.

Acknowledgements
We thank Professor Mark Raftery, Director of the Bioanalytical mass spectrometry facility, University of New South Wales, for in-gel peptide digest and Nano LC-MS sequencing.

Competing interests
The authors declare no competing or financial interests.

Author contributions
N.T. and T.F. conceived and coordinated the study. H.A. performed and analysed the experiments shown in Figs 1–4, 6 and 7. H.A. performed PCR and real-time PCR experiments related to Fig. S3. T.L. produced recombinant Nogo 66 and performed plate-based binding assays and co-immunoprecipitation shown in Fig. 1. M.B. isolated all the fetal primary mouse cortical neurons. B.H., G.J.G. and C.L.G. designed and performed all experiments related to human cortical neurons shown on Fig. 5 and Fig. S3. N.T. and K.B. performed the mass spectrometry (Fig. S1). H.A., N.T. and C.L.G. wrote the paper. K.B. and M.S.L. performed analysed SPR data. E.K. wrote the custom software program used to quantify neurite outgrowth and synapses, quantified and analysed data, designed the illustrations in Figs 3 and 8. All authors reviewed the results and approved the final version of the manuscript.

Funding
This work was supported by the National Health and Medical Research Council of Australia [grant number 568771]; and the Rebecca L. Cooper Foundation. E.K. is a UNSW Vice-Chancellors Research Fellow.

Supplementary information
Supplementary information available online at
http://jcs.biologists.org/lookup/suppl/doi:10.1242/jcs.182006/-/DC1

References
Adelson, J. D., Barreto, G. E., Xu, L., Kim, T., Brott, B. K., Ouyang, Y.-B., Naserke, T., Djurisic, M., Xiong, X., Shatz, C. J. et al. (2012). Neuroprotection from stroke in the absence of MHCI or PirB. *Neuron* **73**, 1100-1107.

An, H., Chandra, V., Piraino, B., Borges, L., Geczy, C., McNeil, H. P., Bryant, K. and Tedla, N. (2010). Soluble LILRA3, a potential natural antiinflammatory protein, is increased in patients with rheumatoid arthritis and is tightly regulated by interleukin 10, tumor necrosis factor-alpha, and interferon-gamma. *J. Rheumatol.* **37**, 1596-1606.

Atwal, J. K., Pinkston-Gosse, J., Syken, J., Stawicki, S., Wu, Y., Shatz, C. and Tessier-Lavigne, M. (2008). PirB is a functional receptor for myelin inhibitors of axonal regeneration. *Science* **322**, 967-970.

Borges, L. and Cosman, D. (2000). LIRs/ILTs/MIRs, inhibitory and stimulatory Ig-superfamily receptors expressed in myeloid and lymphoid cells. *Cytokine Growth Factor Rev.* **11**, 209-217.

Brown, D., Trowsdale, J. and Allen, R. (2004). The LILR family: modulators of innate and adaptive immune pathways in health and disease. *Tissue Antigens* **64**, 215-225.

Chen, M. S., Huber, A. B., van der Haar, M. E., Frank, M., Schnell, L., Spillmann, A. A., Christ, F. and Schwab, M. E. (2000). Nogo-A is a myelin-associated neurite outgrowth inhibitor and an antigen for monoclonal antibody IN-1. *Nature* **403**, 434-439.

Colonna, M., Samaridis, J., Cella, M., Angman, L., Allen, R. L., O'Callaghan, C. A., Dunbar, R., Ogg, G. S., Cerundolo, V. and Rolink, A. (1998). Human myelomonocytic cells express an inhibitory receptor for classical and nonclassical MHC class I molecules. *J. Immunol.* **160**, 3096-3100.

Cosman, D., Fanger, N., Borges, L., Kubin, M., Chin, W., Peterson, L. and Hsu, M.-L. (1997). A novel immunoglobulin superfamily receptor for cellular and viral MHC class I molecules. *Immunity* **7**, 273-282.

Curthoys, N. M., Freittag, H., Connor, A., Desouza, M., Brettle, M., Poljak, A., Hall, A., Hardeman, E., Schevzov, G., Gunning, P. W. et al. (2014). Tropomyosins induce neuritogenesis and determine neurite branching patterns in B35 neuroblastoma cells. *Mol. Cell. Neurosci.* **58**, 11-21.

David, S., Fry, E. J. and López-Vales, R. (2008). Novel roles for Nogo receptor in inflammation and disease. *Trends Neurosci.* **31**, 221-226.

Du, Y., Cui, Y., Liu, X., Hu, F., Yang, Y., Wu, X., Liu, X., Ma, X., Zuo, X., Sheng, Y. et al. (2014). Contribution of functional LILRA3, but not nonfunctional LILRA3, to sex bias in susceptibility and severity of anti-citrullinated protein antibody-positive rheumatoid arthritis. *Arthritis Rheumatol.* **66**, 822-830.

Fath, T., Ke, Y. D., Gunning, P., Götz, J. and Ittner, L. M. (2009). Primary support cultures of hippocampal and substantia nigra neurons. *Nat. Protoc.* **4**, 78-85.

Flanagan, J. G. and Leder, P. (1990). The kit ligand: a cell surface molecule altered in steel mutant fibroblasts. *Cell* **63**, 185-194.

Fournier, A. E., GrandPre, T. and Strittmatter, S. M. (2001). Identification of a receptor mediating Nogo-66 inhibition of axonal regeneration. *Nature* **409**, 341-346.

Fournier, A. E., Takizawa, B. T. and Strittmatter, S. M. (2003). Rho kinase inhibition enhances axonal regeneration in the injured CNS. *J. Neurosci.* **23**, 1416-1423.

Fry, E. J., Ho, C. and David, S. (2007). A role for Nogo receptor in macrophage clearance from injured peripheral nerve. *Neuron* **53**, 649-662.

Fujita, Y., Endo, S., Takai, T. and Yamashita, T. (2011a). Myelin suppresses axon regeneration by PIR-B/SHP-mediated inhibition of Trk activity. *EMBO J.* **30**, 1389-1401.

Fujita, Y., Takashima, R., Endo, S., Takai, T. and Yamashita, T. (2011b). The p75 receptor mediates axon growth inhibition through an association with PIR-B. *Cell Death Dis.* **2**, e198.

Gaus, K., Dean, R. T., Kritharides, L. and Jessup, W. (2001). Inhibition of cholesterol efflux by 7-ketocholesterol: comparison between cells, plasma membrane vesicles, and liposomes as cholesterol donors. *Biochemistry* **40**, 13002-13014.

GrandPré, T., Nakamura, F., Vartanian, T. and Strittmatter, S. M. (2000). Identification of the Nogo inhibitor of axon regeneration as a Reticulon protein. *Nature* **403**, 439-444.

Guillemin, G. J., Smythe, G., Takikawa, O. and Brew, B. J. (2005). Expression of indoleamine 2,3-dioxygenase and production of quinolinic acid by human microglia, astrocytes, and neurons. *Glia* **49**, 15-23.

Guillemin, G. J., Cullen, K. M., Lim, C. K., Smythe, G. A., Garner, B., Kapoor, V., Takikawa, O. and Brew, B. J. (2007). Characterization of the kynurenine pathway in human neurons. *J. Neurosci.* **27**, 12884-12892.

Hartgroves, L. C., Lin, J., Langen, H., Zech, T., Weiss, A. and Harder, T. (2003). Synergistic assembly of linker for activation of T cells signaling protein complexes in T cell plasma membrane domains. *J. Biol. Chem.* **278**, 20389-20394.

Jones, D. C., Kosmoliaptsis, V., Apps, R., Lapaque, N., Smith, I., Kono, A., Chang, C., Boyle, L. H., Taylor, C. J., Trowsdale, J. et al. (2011). HLA class I allelic sequence and conformation regulate leukocyte Ig-like receptor binding. *J. Immunol.* **186**, 2990-2997.

Kabalak, G., Dobberstein, S. B., Matthias, T., Reuter, S., The, Y.-H., Dörner, T., Schmidt, R. E. and Witte, T. (2009). Association of immunoglobulin-like transcript 6 deficiency with Sjögren's syndrome. *Arthritis Rheum.* **60**, 2923-2925.

Kim, T., Vidal, G. S., Djurisic, M., William, C. M., Birnbaum, M. E., Garcia, K. C., Hyman, B. T. and Shatz, C. J. (2013). Human LilrB2 is a beta-amyloid receptor and its murine homolog PirB regulates synaptic plasticity in an Alzheimer's model. *Science* **341**, 1399-1404.

Klotzsch, E., Smorodchenko, A., Löfler, L., Moldzio, R., Parkinson, E., Schütz, G. J. and Pohl, E. E. (2015). Superresolution microscopy reveals spatial separation of UCP4 and F0F1-ATP synthase in neuronal mitochondria. *Proc. Natl. Acad. Sci. USA* **112**, 130-135.

Koch, S., Goedde, R., Nigmatova, V., Epplen, J. T., Müller, N., de Seze, J., Vermersch, P., Momot, T., Schmidt, R. E. and Witte, T. (2005). Association of multiple sclerosis with ILT6 deficiency. *Genes Immun.* **6**, 445-447.

Kritz, A. B., Yu, J., Wright, P. L., Wan, S., George, S. J., Halliday, C., Kang, N., Sessa, W. C. and Baker, A. H. (2008). In vivo modulation of Nogo-B attenuates neointima formation. *Mol. Ther.* **16**, 1798-1804.

Lauren, J., Hu, F., Chin, J., Liao, J., Airaksinen, M. S. and Strittmatter, S. M. (2007). Characterization of myelin ligand complexes with neuronal Nogo-66 receptor family members. *J. Biol. Chem.* **282**, 5715-5725.

Lee, T. H. Y., Mitchell, A., Liu Lau, S., An, H., Rajeaskariah, P., Wasinger, V., Raftery, M., Bryant, K. and Tedla, N. (2013). Glycosylation in a mammalian expression system is critical for the production of functionally active leukocyte immunoglobulin-like receptor A3 protein. *J. Biol. Chem.* **288**, 32873-32885.

Maeda, A., Scharenberg, A. M., Tsukada, S., Bolen, J. B., Kinet, J.-P. and Kurosaki, T. (1999). Paired immunoglobulin-like receptor B (PIR-B) inhibits BCR-induced activation of Syk and Btk by SHP-1. *Oncogene* **18**, 2291-2297.

Martin, A. M., Kulski, J. K., Witt, C., Pontarotti, P. and Christiansen, F. T. (2002). Leukocyte Ig-like receptor complex (LRC) in mice and men. *Trends Immunol.* **23**, 81-88.

Matsushita, H., Endo, S., Kobayashi, E., Sakamoto, Y., Kobayashi, K., Kitaguchi, K., Kuroki, K., Soderhall, A., Maenaka, K., Nakamura, A. et al. (2011). Differential but competitive binding of Nogo protein and class i major histocompatibility complex (MHCI) to the PIR-B ectodomain provides an inhibition of cells. *J. Biol. Chem.* **286**, 25739-25747.

Melrose, J., Roughley, P., Knox, S., Smith, S., Lord, M. and Whitelock, J. (2006). The structure, location, and function of perlecan, a prominent pericellular proteoglycan of fetal, postnatal, and mature hyaline cartilages. *J. Biol. Chem.* **281**, 36905-36914.

Nash, M., Pribiag, H., Fournier, A. E. and Jacobson, C. (2009). Central nervous system regeneration inhibitors and their intracellular substrates. *Mol. Neurobiol.* **40**, 224-235.

Ordóñez, D., Sánchez, A. J., Martínez-Rodríguez, J. E., Cisneros, E., Ramil, E., Romo, N., Moraru, M., Munteis, E., López-Botet, M., Roquer, J. et al. (2009).

Journal of Cell Science

Multiple sclerosis associates with LILRA3 deletion in Spanish patients. *Genes Immun.* **10**, 579-585.

Prinjha, R., Moore, S. E., Vinson, M., Blake, S., Morrow, R., Christie, G., Michalovich, D., Simmons, D. L. and Walsh, F. S. (2000). Neurobiology: Inhibitor of neurite outgrowth in humans. *Nature* **403**, 383-384.

Rodriguez-Feo, J. A., Hellings, W. E., Verhoeven, B. A., Moll, F. L., de Kleijn, D. P. V., Prendergast, J., Gao, Y., van der Graaf, Y., Tellides, G., Sessa, W. C. et al. (2007). Low levels of Nogo-B in human carotid atherosclerotic plaques are associated with an atheromatous phenotype, restenosis, and stenosis severity. *Arterioscler. Thromb. Vasc. Biol.* **27**, 1354-1360.

Schwab, M. E. (2004). Nogo and axon regeneration. *Curr. Opin. Neurobiol.* **14**, 118-124.

Schwab, M. E. (2010). Functions of Nogo proteins and their receptors in the nervous system. *Nat. Rev. Neurosci.* **11**, 799-811.

Shiroishi, M., Tsumoto, K., Amano, K., Shirakihara, Y., Colonna, M., Braud, V. M., Allan, D. S. J., Makadzange, A., Rowland-Jones, S., Willcox, B. et al. (2003). Human inhibitory receptors Ig-like transcript 2 (ILT2) and ILT4 compete with CD8 for MHC class I binding and bind preferentially to HLA-G. *Proc. Natl. Acad. Sci. USA* **100**, 8856-8861.

Syken, J., Grandpre, T., Kanold, P. O. and Shatz, C. J. (2006). PirB restricts ocular-dominance plasticity in visual cortex. *Science* **313**, 1795-1800.

Tedla, N., An, H., Borges, L., Vollmer-Conna, U., Bryant, K., Geczy, C. and McNeil, H. P. (2011). Expression of activating and inhibitory leukocyte immunoglobulin-like receptors in rheumatoid synovium: correlations to disease activity. *Tissue Antigens* **77**, 305-316.

Wright, P. L., Yu, J., Di, Y. P. P., Homer, R. J., Chupp, G., Elias, J. A., Cohn, L. and Sessa, W. C. (2010). Epithelial reticulon 4B (Nogo-B) is an endogenous regulator of Th2-driven lung inflammation. *J. Exp. Med.* **207**, 2595-2607.

Zheng, J., Umikawa, M., Cui, C., Li, J., Chen, X., Zhang, C., Hyunh, H., Kang, X., Silvany, R., Wan, X. et al. (2012). Inhibitory receptors bind ANGPTLs and support blood stem cells and leukaemia development. *Nature* **485**, 656-660.